Missouri University of Science and Technology
Scholars' Mine

Chemistry Faculty Research & Creative Works | Chemistry

01 Jun 2019

# Ultrasensitive and Highly Selective $Ni_3Te_2$ as a Nonenzymatic Glucose Sensor at Extremely Low Working Potential

Bahareh Golrokh Amin

Umanga De Silva

Jahangir Masud

Manashi Nath
*Missouri University of Science and Technology*, nathm@mst.edu

Follow this and additional works at: https://scholarsmine.mst.edu/chem_facwork

 Part of the Chemistry Commons

## Recommended Citation

B. Golrokh Amin et al., "Ultrasensitive and Highly Selective $Ni_3Te_2$ as a Nonenzymatic Glucose Sensor at Extremely Low Working Potential," *ACS Omega*, vol. 4, no. 6, pp. 11152-11162, American Chemical Society (ACS), Jun 2019.
The definitive version is available at https://doi.org/10.1021/acsomega.9b01063

This Article - Journal is brought to you for free and open access by Scholars' Mine. It has been accepted for inclusion in Chemistry Faculty Research & Creative Works by an authorized administrator of Scholars' Mine. This work is protected by U. S. Copyright Law. Unauthorized use including reproduction for redistribution requires the permission of the copyright holder. For more information, please contact scholarsmine@mst.edu.

This is an open access article published under an ACS AuthorChoice License, which permits copying and redistribution of the article or any adaptations for non-commercial purposes.

ACS OMEGA

Article

Cite This: ACS Omega 2019, 4, 11152−11162

http://pubs.acs.org/journal/acsodf

# Ultrasensitive and Highly Selective $Ni_3Te_2$ as a Nonenzymatic Glucose Sensor at Extremely Low Working Potential

Bahareh Golrokh Amin, Umanga De Silva, Jahangir Masud, and Manashi Nath*

Department of Chemistry, Missouri University of Science and Technology, Rolla, Missouri 65409, United States

Supporting Information

**ABSTRACT:** Developing Nonenzymatic glucose biosensors has recently been at the center of attention owing to their potential application in implantable and continuous glucose monitoring systems. In this article, nickel telluride nanostructure with the generic formula of $Ni_3Te_2$ has been reported as a highly efficient electrocatalyst for glucose oxidation, functional at a low operating potential. $Ni_3Te_2$ nanostructures were prepared by two synthesis methods, direct electrodeposition on the electrode and hydrothermal method. The electrodeposited $Ni_3Te_2$ exhibited a wide linear range of response corresponding to glucose oxidation exhibiting a high sensitivity of 41.615 mA $cm^{-2}$ $mM^{-1}$ and a low limit of detection (LOD) of 0.43 $\mu$M. The hydrothermally synthesized $Ni_3Te_2$, on the other hand, also exhibits an ultrahigh sensitivity of 35.213 mA $cm^{-2}$ $mM^{-1}$ and an LOD of 0.38 $\mu$M. The observation of high efficiency for glucose oxidation for both $Ni_3Te_2$ electrodes irrespective of the synthesis method further confirms the enhanced intrinsic property of the material toward glucose oxidation. In addition to high sensitivity and low LOD, $Ni_3Te_2$ electrocatalyst also has good selectivity and long-term stability in a 0.1 M KOH solution. Since it is operative at a low applied potential of 0.35 V vs AglAgCl, interference from other electrochemically active species is reduced, thus increasing the accuracy of this sensor.

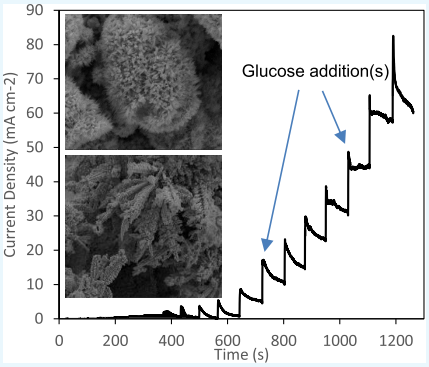


## INTRODUCTION

In the current society, diabetes has rapidly grown to be one of the leading causes of death on a global scale. Diabetes stems from abnormal blood glucose level, and frequent self-monitoring and continuous testing of physiological glucose concentration are key to controlling the advancement of the disease. Continuous blood glucose monitoring allows for better glycemic control, resulting in lesser fluctuation of blood glucose levels in diabetic patients. By better monitoring of the glucose concentration in blood, patients are more likely to prevent the occurrence of diabetic emergencies such as hypoglycemia or hyperglycemia, as well as to avoid long-term complications associated with the disease, such as kidney failure, blindness, and high blood pressure.[1−4] The conventional approach for monitoring the spread of the disease and controlling it involves regular sampling of the blood glucose level via finger pricking, which causes anxiety, tension, and additional pain to the patients. Also, relying on blood samples collected at various times throughout the day under different physiological conditions will provide sporadic results of glucose levels, making this approach less reliable for the purpose of administering insulins.[5,6] Therefore, researchers are trying to develop more convenient glucose sensors, capable of continuously and reproducibly measuring glucose levels at different concentrations.

With the advent of modern monitoring devices, a highly sensitive and accurate glucose measuring system should be able to reliably detect glucose from the blood, as well as alternative biofluids, including saliva, urine, sweat, etc. If diabetic patients are provided with such noninvasive and convenient glucose sensors, they are more likely to measure frequent glucose levels, which will allow them to optimize their insulin injections.[7,8] However, glucose concentrations in these body fluids are as low as 0−0.8 mmol $L^{-1}$ for urine,[9] 0.03−0.08 mmol $L^{-1}$ for saliva,[10] and 0.02−0.6 mmol $L^{-1}$ for sweat,[11] requiring the glucose sensors to be highly sensitive with extremely low limit of detection (LOD) and better selectivity. The rapid response time and precise measurements achievable by electrochemical sensing methods have made glucose detection possible from body fluids other than blood.[12] However, conventionally used enzyme-based glucose sensors still fall short of these requirements since their efficiencies are influenced by changes in pH and variation of temperature in addition to the difficulty of immobilizing fragile enzyme on the electrode surface. The efficiency of enzymatic glucose sensors can also be affected by the presence of other interfering compounds in blood.[13−16] Due to the high working potential required for electron transfer between thick enzyme layer and glucose molecules, other redox-active species present in blood can also oxidize/degrade, thus affecting the accuracy of glucose sensing.[17] According to recent research developments, all of the crucial parameters including sensitivity, selectivity, LOD, and stability can be improved by employing the next-generation glucose sensing modules, namely, the nonenzymatic

Received: April 15, 2019
Accepted: June 10, 2019
Published: June 26, 2019

Downloaded via MISSOURI UNIV SCIENCE & TECHNOLOGY on August 22, 2019 at 17:41:16 (UTC).
See https://pubs.acs.org/sharingguidelines for options on how to legitimately share published articles.


© 2019 American Chemical Society

DOI: 10.1021/acsomega.9b01063
ACS Omega 2019, 4, 11152−11162

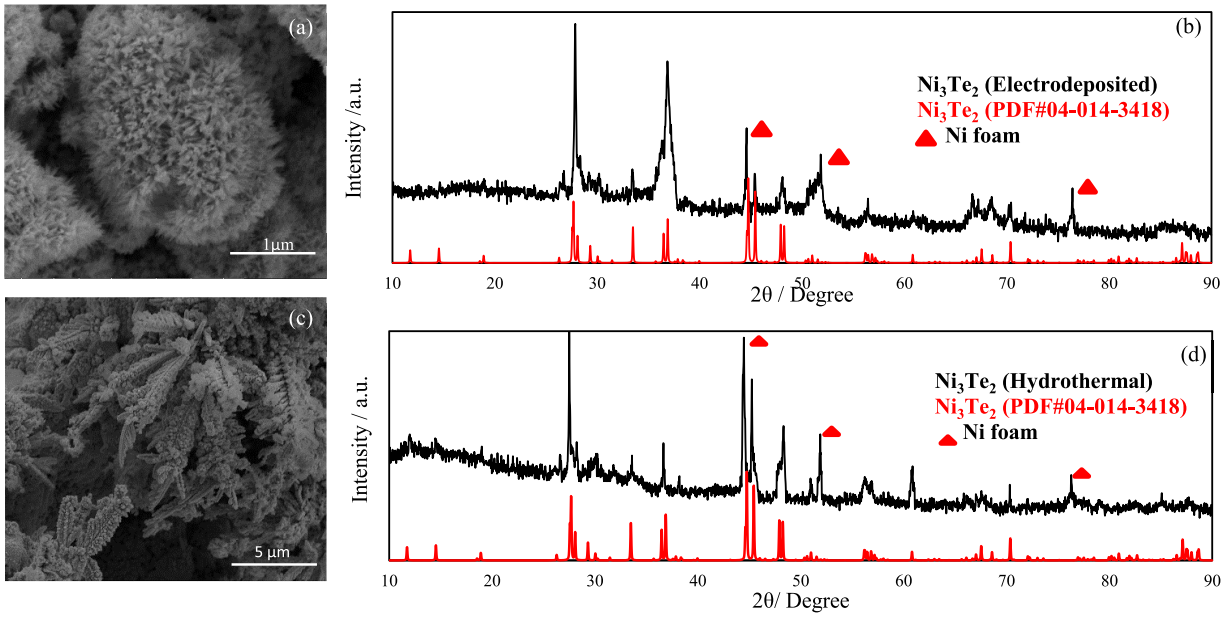


**Figure 1.** Characterization of electrodeposited $Ni_3Te_2$ catalyst: (a) SEM image on Ni foam. (b) Powder X-ray diffraction (PXRD) patterns of electrodeposited $Ni_3Te_2$ on Ni foam. Characterization of hydrothermally synthesized $Ni_3Te_2$. (c) SEM image on $Ni_3Te_2$−NF. (d) PXRD analysis of hydrothermally synthesized $Ni_3Te_2$ catalysts along with the reference (PDF #04-014-3418) pattern.

glucose sensors.[18,19] While enzyme-based sensors are dependent on thick enzymes to mediate electron transfer, in nonenzymatic glucose biosensors, on the other hand, the process of glucose oxidation takes place directly on the electrode surface. Specific glucose oxidation electrocatalysts anchored on the electrode surface facilitate electron-transfer process at the electrode−analyte interface, thereby decreasing the operating potential for glucose oxidation and improving efficiency of the sensor.[20−25]

Among nonenzymatic electrochemical glucose sensors, noble metals such as Au-based,[26−30] Pt-based,[31,32] or Pd-based[33,34] and their alloys exhibit an enhanced conductivity with an accelerated electrochemical redox process for glucose biosensing. However, the scarcity and high cost of these precious metals inhibit their large-scale usage in practical implementations.[35−40] To mitigate this issue, nanocatalysts based on earth-abundant transition metals have received great attention in virtue of their excellent redox behavior, natural abundance, lower cost, functional stability in alkaline medium, and satisfactory biocompatibility.[41−43] Among transition metals, Ni-based catalysts are of interest for electrochemical nonenzymatic glucose sensing owing to their low cost and remarkably high catalytic activity arising from the facile transformation of $Ni^{2+}/Ni^{3+}$ redox couple in alkaline medium, which facilitates the electrooxidation of glucose on the electrode surface.[44−47]

Recent studies by several researchers have shown that nickel chalcogenide-based electrocatalysts possess unprecedented electrochemical activity toward several energy conversion processes such as full water splitting[48−54] and supercapacitors.[55,56] Such enhancement of electrocatalytic activity of the Ni chalcogenides compared to that of their oxide analogue is caused by the facile electrochemical redox of the active Ni center, as well as decreased band gap and increased metallicity of the chalcogenide lattice compared to that of the oxides, which are higher band-gap insulators. The higher conductivity of the lattice also enhances electron-transfer efficiency within transition-metal selenide and telluride composites compared to that in the corresponding oxides. The trend in catalytic activity from the oxides to the other chalcogenide series (sulfides, selenides, and tellurides) can also be explained through their gradual change in the electronegativity of the chalcogen atom. As the electronegativity of the chalcogen atom decreases down the series, the degree of covalency in metal−chalcogen bond increases. Since the electrocatalytic efficiency is enhanced by a higher degree of covalency in metal−anion bonding, it is expected that the catalytic efficiency will increase in the chalcogenide series from oxide to telluride.[48,56] Moreover, the higher applied potentials required for nickel-based oxides decrease the efficiency of these electrodes toward glucose biosensing. Ni chalcogenides, on the other hand, being electrochemically active at a much lower applied potential can significantly increase the catalytic efficiency for direct glucose oxidation.[57,58]

In this study, the electrocatalytic activity of nickel telluride nanostructures with the molecular formula of $Ni_3Te_2$ has been reported for direct glucose oxidation in an alkaline medium. The $Ni_3Te_2$ electrocatalyst composite has been synthesized by two approaches: direct electrodeposition and one-step hydrothermal synthesis. Both of these catalyst composites show similar activity toward the oxidation of glucose to gluconolactone, indicating that it is indeed an intrinsic property for $Ni_3Te_2$ independent of the synthesis method. High sensitivity and low LOD were obtained with the $Ni_3Te_2$ electrocatalyst at low applied potentials for glucose oxidation, making this compound promising for nonenzymatic glucose biosensors.

## RESULTS AND DISCUSSION

**Morphology and Composition.** Scanning electron microscopy (SEM) image of the as-grown electrodeposited films shows randomly oriented nanoflakes on the surface of Ni foam, as shown in Figure 1a. Such a nanoflake geometry expectedly increases the active surface area of the electrocatalyst composite leading to better exposure of the catalytic



DOI: 10.1021/acsomega.9b01063
ACS Omega 2019, 4, 11152−11162

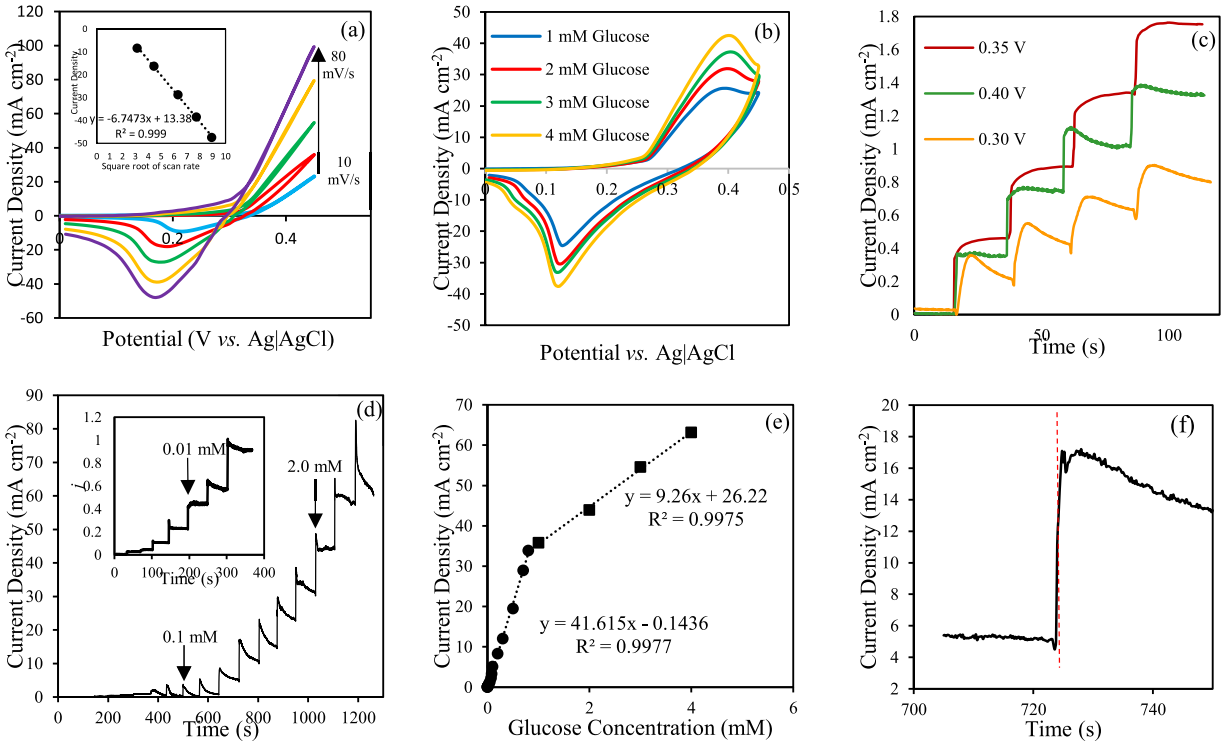


**Figure 2.** (a) Cyclic voltammograms of electrodeposited $Ni_3Te_2$ at different scan rates. The inset shows the cathodic peak currents of electrodeposited $Ni_3Te_2$ electrode vs square root of scan rate. (b) Response of electrodeposited $Ni_3Te_2$−NF electrode in 0.1 M KOH containing 1−4 mM of glucose at a scan rate of 10 mV $s^{-1}$. (c) Effect of various potentials on amperometric response of electrodeposited $Ni_3Te_2$ electrode to the successive addition of 0.01 mM glucose. (d) Amperometric response of electrodeposited $Ni_3Te_2$ upon the addition of different concentrations of glucose at 0.35 V. The inset shows the amperometric response in low glucose concentration. (e) Corresponding calibration curve of the response current density as a function of glucose concentration. (f) Response time of the sensor to achieve steady-state current density upon the addition of glucose.

sites to the analyte present in the electrolyte, thus improving catalytic interaction. SEM image of the hydrothermally synthesized $Ni_3Te_2$, on the other hand, shows leaflike dendritic nanostructures on the electrode surface (Figure 1c). It is worth mentioning that $Ni_3Te_2$ grown on Ni foam both by electrodeposition and by hydrothermal methods shows high surface area amenable for superior catalytic activity. The $Ni_3Te_2$ nanostructures were also analyzed through transmission electron microscopy (TEM), and the results have been included in our previous publication.[48] TEM images show granular particle-like and flake-like morphologies for the hydrothermally synthesized and electrodeposited $Ni_3Te_2$, respectively.

The PXRD patterns of the electrodeposited $Ni_3Te_2$, as well as the hydrothermally synthesized $Ni_3Te_2$ on Ni foam (NF), show the presence of pure $Ni_3Te_2$, where the diffraction peaks matched with those reported for standard $Ni_3Te_2$ (PDF #04-014-3418), as shown in Figure 1b,d. Both PXRD patterns show that the product formed was a pure phase with no other evident impurity peaks. It was also observed that the relative peak intensities and peak widths were different between the hydrothermally synthesized and electrodeposited $Ni_3Te_2$. Such differences can be explained by the smaller nanostructures in the electrodeposited sample, which causes broadening of the diffraction peak, and possible oriented growth in the electrodeposited film, which has been previously observed for $NiSe_2$.[51]

**Electrochemical Measurements.** Cyclic voltammetry (CV) and chronoamperometry measurements were performed with an Iviumstat potentiostat under continuous stirring in a three-electrode electrochemical setup, where $Ni_3Te_2$−NF served as the working electrode, while a platinum mesh and Ag|AgCl electrode were selected as the counter and reference electrodes, respectively. An aqueous 0.1 M KOH solution was used as the electrolyte.

The limit of detection (LOD) was calculated according to the following equation (eq 1)[59−61]

$$\mathrm{LOD} = \frac{3\mathrm{SD}}{N} \tag{1}$$

where SD is the standard deviation of the analyte concentration calculated from the current response of the consecutive addition of glucose into the electrolyte and $N$ is the slope of the calibration curve, which indicates the sensitivity of the electrode with a signal-to-noise ratio of 3.

The electrochemical active surface area (ECSA) was estimated by measuring the double-layer charging current at different scan rates based on the following equation (eq 2)[49]

$$\mathrm{ECSA} = \frac{C_{\mathrm{DL}}}{C_s} \tag{2}$$

where $C_s$ is the specific capacitance (0.040 mF $cm^{-2}$) in a $N_2$-saturated 0.1 M KOH solution and $C_{DL}$ is the double-layer capacitance calculated from the slope of the plot of capacitive current ($i_{DL}$) in a nonfaradic double-layer region against scan rate v (V $s^{-1}$). The ECSA was measured to be 13.0 $cm^2$ for electrodeposited $Ni_3Te_2$ and 20.2 $cm^2$ for hydrothermally



DOI: 10.1021/acsomega.9b01063
ACS Omega 2019, 4, 11152−11162

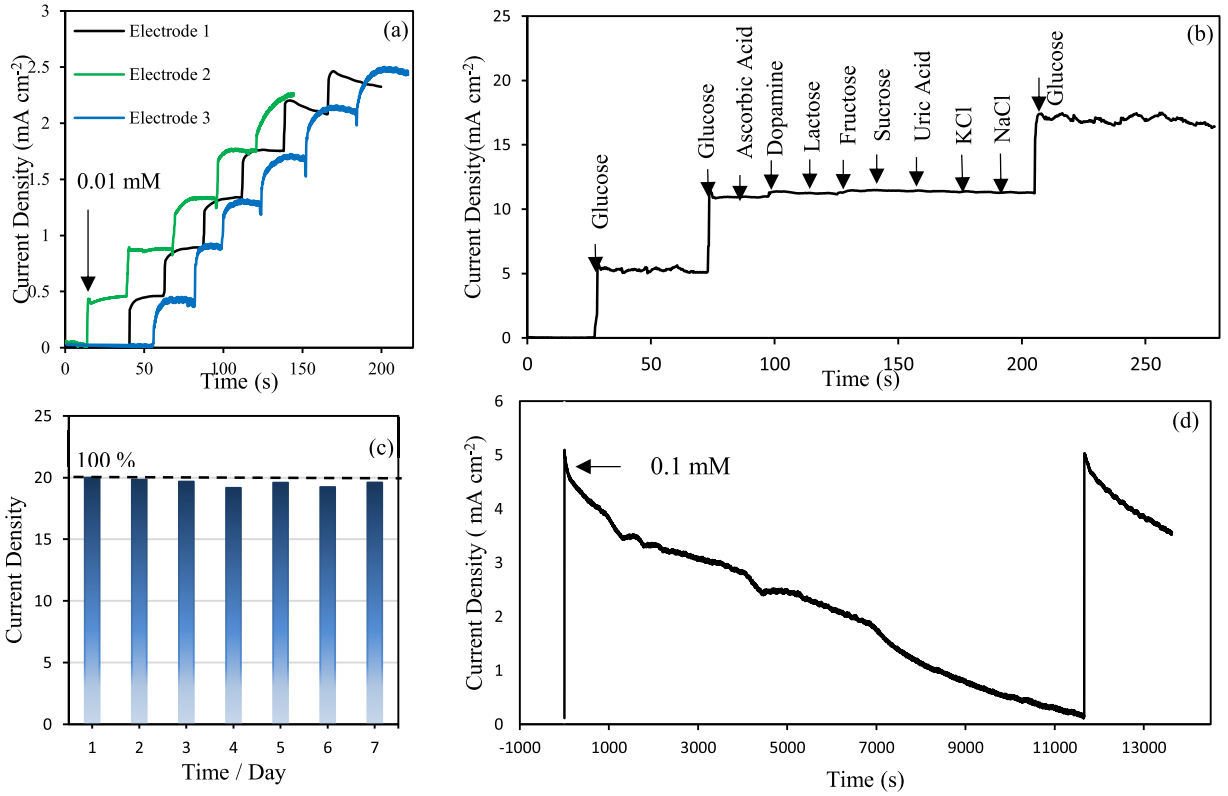


**Figure 3.** (a) Amperometric response of electrodeposited $Ni_3Te_2$ to the successive addition of 0.01 mM glucose at 0.35 V. (b) Interference assessment performance of the electrodeposited $Ni_3Te_2$ upon the addition of 0.1 mM glucose and 0.01 mM of interfering species, as identified in the diagram. (c) Long-term stability check of the electrode measured for 7 days. (d) Prolonged chronoamperometry test with the addition of 0.1 mM glucose to 0.1 M KOH.

synthesized $Ni_3Te_2$, as shown in the Supporting Information (Figures S1 and S2, respectively).

**Electrochemical Behavior of Electrodeposited $Ni_3Te_2$–NF Electrode.** Cyclic voltammetry (CV) is known to be useful for investigating the electrochemical behavior of the electrode. The CV plots and influence of the scan rate on the current density of electrodeposited $Ni_3Te_2$ in 0.1 M KOH in the absence of glucose are provided in Figure 2a. As shown in Figures 2a and S1, by increasing the scan rate from 10 to 80 mV $s^{-1}$, the current density changes proportionally with the square root of scan rate, implying a typical diffusion-controlled electrochemical process at the surface of the electrode.

The CV response of electrodeposited $Ni_3Te_2$–NF electrode in the presence of different concentrations of glucose in the electrolyte is presented in Figure 2b. It can be seen from this figure that an explicit oxidation peak located at 0.35 V vs Agl AgCl was observed in the presence of glucose with concentrations ranging from 1 to 4 mM. The enhancement of anodic peak current densities was more obvious with the increase of glucose concentration, suggesting high electrocatalytic activity of electrodeposited $Ni_3Te_2$ toward glucose electrooxidation. It is worth mentioning that upon the addition of 1.0 mM glucose, bare Ni foam did not show any oxidation peak corresponding to glucose oxidation in the working potential ranging from 0 to 0.5 V vs AglAgCl (Figure S3), confirming that the substrate by itself was not an active electrocatalyst for glucose oxidation.

The large current densities achieved by electrodeposited $Ni_3Te_2$ electrode in the presence of a 4 mM glucose concentration, reveal another potential application of this electrode in a nonenzymatic glucose fuel cell.[62] Currently, the development of implantable medical devices has been limited due to the slow improvements in lithium-ion battery technology. Glucose fuel cells are potential candidates to replace the lithium-ion batteries due to their superior long-term stability, sufficient power density, and abundance of glucose in the body to generate a continuous and stable power output. However, the main challenge for enzymatic glucose fuel cells is the poor anode selectivity toward glucose oxidation in the presence of oxygen in the body tissue.[63−65] Non-enzymatic glucose fuel cell with a high current response and excellent selectivity can be a feasible solution for improvements in power generation for implantable medical devices. It can be concluded from Figure 2b that electrodeposited $Ni_3Te_2$ can be a potential choice for this technology, as it shows a high current density of about 45 mA $cm^{-2}$ in the presence of 4 mM glucose.

**Electrocatalytic Oxidation of Glucose on Electrodeposited $Ni_3Te_2$.** A high amperometric current response during detection of glucose can be strongly affected by the applied potential. Large applied potential can trigger oxygen evolution reaction at the anode, which leads to a large background anodic current and dwindling of the active surface area.[66] Therefore, to determine the optimum working potential for glucose sensing, the amperometric response of the $Ni_3Te_2$–NF electrode was recorded at different applied potentials. As Figure 2c shows, with the successive addition of 0.01 mM of glucose into a 0.1 M KOH solution, the catalytic current of electrodeposited $Ni_3Te_2$–NF electrode elevated with the increase of applied potential from 0.30 to 0.35 V but then



DOI: 10.1021/acsomega.9b01063
ACS Omega 2019, 4, 11152−11162

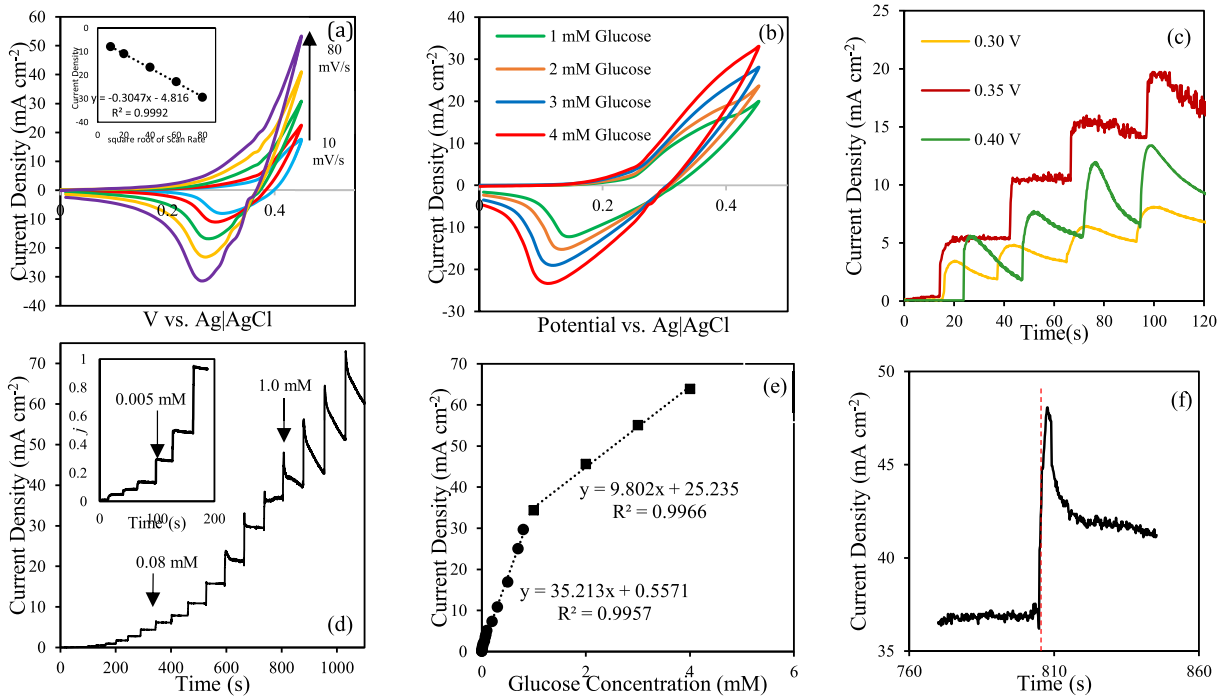


**Figure 4.** (a) CVs of the hydrothermally synthesized $Ni_3Te_2$ in a 0.1 M KOH medium at various scan rates (10−80 mV $s^{-1}$). The inset shows the cathodic peak currents of hydrothermally synthesized $Ni_3Te_2$−NF electrodes as a function of the square root of scan rate. (b) CVs of the hydrothermally prepared $Ni_3Te_2$ electrode with glucose concentration increased from 1 to 4 mM. (c) Amperometric responses at different working potentials ranging from 0.30 to 0.40 V to the successive addition of 0.1 mM glucose to 0.1 M KOH. (d) Amperometric response of the hydrothermally synthesized $Ni_3Te_2$ at 0.35 V to the stepwise addition of different concentrations of glucose. The inset shows the zoomed-in response of the electrode at lower glucose concentration. (e) Corresponding calibration curve of response current density vs glucose concentration. (f) Response time of the electrode to glucose oxidation.

decays at 0.40 V potential. Therefore, 0.35 V vs Ag|AgCl was selected as the optimal applied potential for electrodeposited $Ni_3Te_2$ electrode, which enables the best sensing performance for glucose oxidation. It should be noted here that this is one of the lowest potentials reported for electrocatalytic glucose oxidation and is much lower than that of oxide-based sensors. The onset of electrocatalytic glucose oxidation at such low working potential validates our initial hypothesis and confirms that replacing oxides by chalcogenides such as selenides and tellurides enhances electrode activation at lower potential and will result in a high selectivity of the electrode.[67] Additionally, the reduced band gap in selenides and tellurides also leads to better electrical conductivity and charge transfer in the catalyst composite, leading to high current densities at low applied potentials.

The mechanism of glucose oxidation is believed to be initiated by the hydroxyl attachment on the catalytically active transition-metal site, Ni(III), which is generated in situ through local site oxidation of Ni(II) (catalyst activation). The electron transfer is then initiated between the glucose molecule and the hydroxyl-activated catalytic site, leading to glucose oxidation to gluconolactone and further redox of the transition-metal catalytic site.[68] Since the catalytically active transition-metal site undergoes a reversible oxidation−reduction cycle during the mechanism of glucose oxidation, the redox potential for the transition-metal sites can have a large influence on the catalytic efficiency for glucose oxidation, especially the applied potential value. Previous research from our group has shown that the $Ni^{2+}/Ni^{3+}$ redox potential can be shifted to more cathodic potential in $Ni_3Te_2$ compared to Ni oxides,[48] thereby reducing the applied potential for catalyst activation.

The amperometric response of the electrodeposited $Ni_3Te_2$−NF was measured at a constant applied potential of 0.35 V with successive addition of different concentrations of glucose into the alkaline solution under continuous stirring and is shown in Figure 2d. The inset shows the magnified version of the amperometric response at low glucose concentrations. As can be seen from these plots, the current response illustrated a high sensitivity of the electrode to glucose concentration as low as 0.01 $\mu$M, which can easily be detected by electrodeposited $Ni_3Te_2$ electrode. The calibration curve shown in Figure 2e, obtained by plotting the steady-state current density values vs the glucose concentrations, reveals two linear regions. In the low-glucose-concentration ranges from 0.01 $\mu$M to 0.8 mM, the response is linear with an ultrahigh sensitivity of 41.615 mA $mM^{-1}$ $cm^{-2}$ ($R^2$ = 0.9977). While the second linear region between 1 and 4 mM shows a sensitivity of 9.26 mA $mM^{-1}$ $cm^{-2}$ ($R^2$ = 0.9975). For the linear range from 0.01 $\mu$M to 0.8 mM, based on eq 1, the LOD was estimated to be 0.43 $\mu$M with a signal-to-noise ratio of 3 (S/N = 3).

As can be seen from Figure 2f, a rapid current response was achieved upon the addition of glucose, reaching the steady-state current in less than 2 s. The fast response time demonstrates competent activity of electrodeposited $Ni_3Te_2$ electrode toward glucose sensing.

Figure 3a shows the amperometric responses of electrodeposited $Ni_3Te_2$ to stepwise injections of 0.01 mM of glucose to 0.1 M KOH at 0.35 V, wherein current response from different batches of electrodes were measured under



DOI: 10.1021/acsomega.9b01063
ACS Omega 2019, 4, 11152−11162

identical experimental conditions. It was observed that the addition of a similar concentration of glucose resulted in almost identical jumps in current density. This repeatability of the results confirms the reliability of $Ni_3Te_2$ as a sensor, as well as its functional stability in an alkaline medium, along with reproducibility of the results.

For an electrochemical glucose sensor, selectivity is a crucial feature to assess the ability of the electrode to be utilized in practical applications. Normally, certain biomolecules such as ascorbic acid, fructose, sucrose, and lactose coexist with glucose in human blood. These interfering species may also undergo electrochemical oxidation, thus producing background current signal at high applied potentials, which will affect the accurate determination of glucose concentration. Hence, an experiment was conducted for examining the selectivity of the electrodeposited $Ni_3Te_2$−NF electrode, where the amperometric current response of electrodeposited $Ni_3Te_2$ to the sequential addition of 0.1 mM of glucose and 0.01 mM of a number of interfering compounds including ascorbic acid, dopamine, lactose, fructose, sucrose, uric acid, KCl, and NaCl was measured at an applied potential of 0.35 V vs AgIAgCl, and the results are shown in Figure 3b. It is clearly seen that the electrochemical signals from interferant species are negligible compared to the significant jump of current density observed with the addition of glucose, confirming superior selectivity of $Ni_3Te_2$ electrode towards glucose oxidation.

Long-term stability and repeatability of the $Ni_3Te_2$−NF electrode towards glucose sensing were estimated by checking the electrode response to the addition of similar concentration of glucose over a week where the electrode was stored under ambient conditions and reused. Figure 3c shows the results of these tests, and it can be clearly seen that the electrode produced similar response throughout, indicating stability and repeatability of the sensor. Even after being exposed to air for 7 days, electrodeposited $Ni_3Te_2$ retained at least 96% of its original current response.

The reproducibility of the electrode toward glucose oxidation was also tested by adding 0.1 mM of glucose to 0.1 M KOH under constant stirring. After almost 3 h, electrodeposited $Ni_3Te_2$ completely oxidized all of the added glucose, reducing the current density to nearly zero. Fresh addition of 0.1 mM of glucose at this point immediately increased the current density to a value almost similar to the previous value, as shown in Figure 3d, confirming the reproducibility of the current response of the sensor.

**Electrochemical Behavior of Hydrothermally Synthesized $Ni_3Te_2$.** Hydrothermally synthesized $Ni_3Te_2$ was assembled on the electrode surface, as discussed above. Similar to electrodeposited $Ni_3Te_2$, hydrothermally synthesized $Ni_3Te_2$ was also tested for glucose sensing in 0.1 M KOH by collecting CV scans in the absence and presence of glucose. The CV plots shown in Figure 4a represent the current response in the absence of glucose and were performed in the potential range from 0 to +0.45 V vs AgIAgCl with scan rates increasing from 10 to 80 mV $s^{-1}$. The cathodic current measured was proportional to the square root of scan rate, as shown in the inset, suggesting a typical diffusion-controlled process for the hydrothermally prepared $Ni_3Te_2$ electrode.

Upon the addition of different concentrations of glucose ranging from 1 to 4 mM, a notable enhancement of the anodic current density was observed, while the peak oxidation potential stayed at almost the same position, demonstrating the electrode's activity toward glucose oxidation. It is well established that the enhancement of the oxidative current is attributed to the electrooxidation of glucose in the presence of Ni(III).[69]

The high current density of almost 30 mA $cm^{-2}$ is achieved by the hydrothermally prepared $Ni_3Te_2$ in the presence of 4 mM glucose. This result shows that the hydrothermally prepared $Ni_3Te_2$ electrodes, similar to those made through electrodeposition, have the potential of being used in devices for energy conversion from glucose.

**Glucose Oxidation with Hydrothermally Prepared $Ni_3Te_2$.** As mentioned above, applied potential can strongly affect the magnitude of current response for the glucose sensor. Therefore, we have analyzed the current response with respect to variations in the applied potential to select an optimal potential. Figure 4c shows the amperometric responses of hydrothermally synthesized $Ni_3Te_2$ to the sequential addition of 0.1 mM of glucose at different applied potentials ranging from 0.30 to 0.40 V. Based on the observed current response, the optimal potential for amperometric detection of glucose was selected to be 0.35 V vs AgIAgCl, which aligns with CV results mentioned above.

Amperometric response upon successive addition of different concentrations of glucose into a constantly stirred 0.1 M KOH solution was measured at 0.35 V and is shown in Figure 4d. In this figure, distinct increases in amperometric currents were observed with the stepwise increase of added glucose concentration, demonstrating superior catalytic ability of hydrothermally prepared $Ni_3Te_2$ electrode for glucose electrooxidation. The inset shows current response of the sensor in the region of low added-glucose concentrations, confirming the ability of the sensor to reliably detect even minute amounts of glucose, which leads to high sensitivity of the electrode toward glucose electrooxidation.

The amperometric current response with the addition of varying amounts of glucose was used to obtain the calibration curve, as shown in Figure 4e. It was observed that there were two linear regions in the calibration curve, one at the lower glucose concentration (up to 0.8 mM) and the other at the higher glucose concentration (1−4 mM). The linear fit in the low-glucose-concentration region (0.01−0.8 mM) showed an ultrahigh sensitivity of 35.213 mA $mM^{-1}$ $cm^{-2}$ ($R^2$ = 0.9957). The LOD was as low as 0.38 $\mu$M, based on the signal/noise value of 3 (S/N = 3). The sensitivity in the higher glucose concentration from 1.0 to 4.0 mM was calculated to be 9.802 mA $mM^{-1}$ $cm^{-2}$ ($R^2$ = 0.9966). At higher glucose concentration, the amperometric current density gradually reaches a saturation due to the presence of adsorbed reaction intermediates on the electrode surface covering the available active sites. This may lead to insufficient active sites to oxidize the incoming glucose on the electrode surface. The addition of glucose in the vicinity of the electrode produces a sharp increase in current density with a response time of less than 4 s, as can be seen in Figure 4f. Such low response time verifies the high catalytic activity of hydrothermally prepared $Ni_3Te_2$ toward glucose oxidation. The $Ni_3Te_2$ electrodes were also analyzed through electroimpedance spectroscopy (EIS), and from the fitting of the EIS spectra (as shown in Figure S4), the $R_{ct}$ (charge-transfer resistance) values were estimated to be 45.38 Ω for electrodeposited $Ni_3Te_2$ and 45.98 Ω for hydrothermal $Ni_3Te_2$. Such small charge-transfer resistances are indicative of fast charge-transfer kinetics at the electrode−electrolyte interface and low contact resistance.



DOI: 10.1021/acsomega.9b01063
ACS Omega 2019, 4, 11152−11162

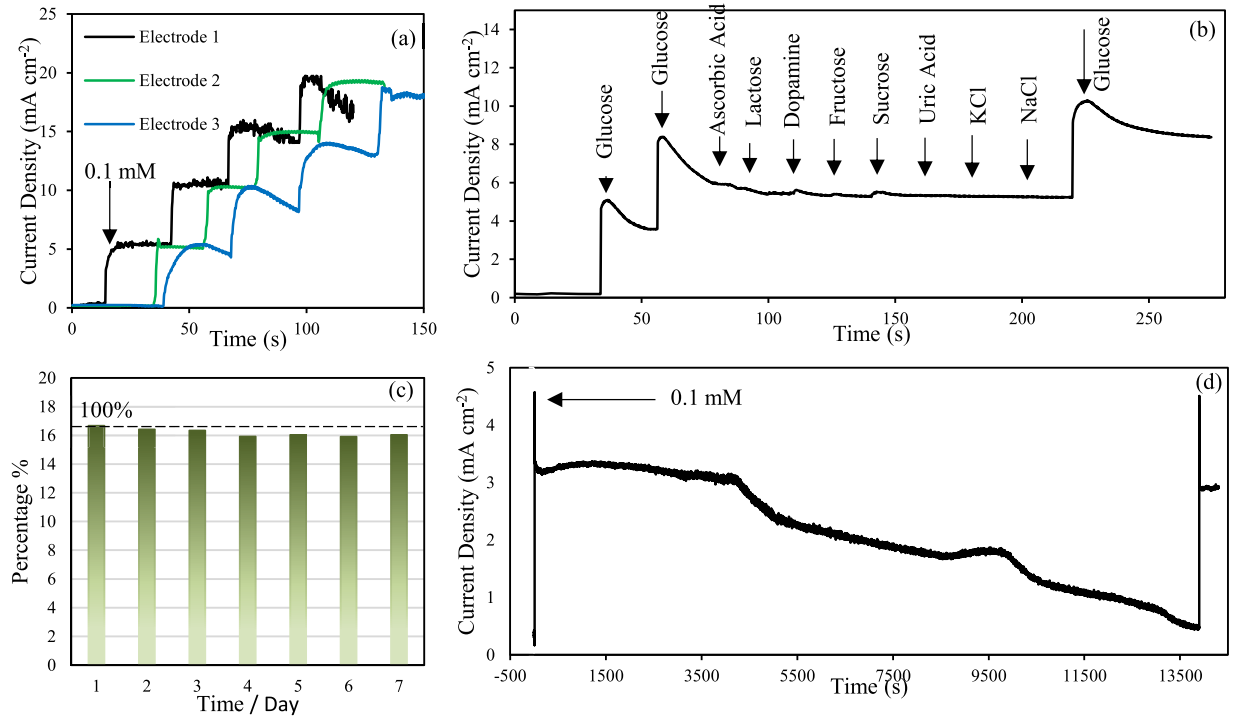


**Figure 5.** (a) Amperometric response of different batches of hydrothermally synthesized $Ni_3Te_2$–NF electrodes to the stepwise addition of similar concentrations of glucose in an alkaline solution. (b) Amperometric response of the electrode to the addition of glucose (0.1 mM) and other interfering species (0.01 mM), as mentioned in the diagram. (c) Extensive stability check of the $Ni_3Te_2$–NF electrode measured for 7 days. (d) Continuous chronoamperometric test to the addition of identical concentrations of glucose, as well as the complete oxidation time.

The reproducibility of the results, as well as the reliability of these measurements, was tested by measuring the electrochemical response from several electrodes assembled from different batches of hydrothermally synthesized $Ni_3Te_2$. It was observed that the different electrodes showed an almost identical jump in current densities with the addition of same concentrations of glucose (0.1 mM) in 0.1 M KOH at 0.35 V vs Ag|AgCl, as shown in Figure 5a. Such an identical current response between different electrodes and different addition events confirmed the excellent stability and reproducibility of these electrodes.

One of the major challenges in nonenzymatic glucose sensing, as mentioned above, is to eliminate the interference from biomolecules coexisting in the blood such as dopamine, ascorbic acid, urea, salts, fructose, etc. In physiological conditions, the level of glucose is much higher than that of these interfering species (<0.5 mM).[64,66] Hence, the selectivity of the hydrothermally synthesized $Ni_3Te_2$–NF electrode was determined toward glucose oxidation in the presence of added interferent species by measuring the current response upon the addition of 0.1 mM of glucose followed by successive additions of 0.01 mM of ascorbic acid, dopamine, lactose, fructose, sucrose, uric acid, KCl, and NaCl, as shown in Figure 5b. It was found that the hydrothermally prepared $Ni_3Te_2$ electrode provides remarkable response only for glucose electrooxidation, while the addition of other species had a negligible effect on the anodic current.

The long-term stability of this nonenzymatic sensor was also evaluated through amperometric response for the specific concentration of glucose recorded for over a week (Figure 5c). The hydrothermally prepared $Ni_3Te_2$ electrode was stored in air when not in use and was reused for this study. The results indicate that the sensor retained more than 94% of its initial current response, suggesting favorable long-term stability and reproducibility of this nonenzymatic glucose sensor.

To investigate the cyclability of the hydrothermally prepared $Ni_3Te_2$ electrode, a chronoamperometry experiment was carried out, where 0.1 mM glucose was injected into 0.1 M of KOH at 0.35 V and the oxidation current was allowed to decay down, indicating full oxidation of the added glucose. This electrode needed almost 5 h to convert all of the added glucose to gluconolactone. Glucose solution (0.1 mM) was added again to this electrolyte, which resulted in similar current density as the initial addition of glucose (Figure 5d), confirming data reliability and reproducibility for long-term tests.

The $Ni_3Te_2$ electrode was also analyzed through SEM and PXRD to investigate the structural and compositional stability after a prolonged period of glucose oxidation. SEM analysis showed that both hydrothermally synthesized and electrodeposited $Ni_3Te_2$ maintained their respective morphologies after chronoamperometric test, as shown in Figure S5 in the Supporting Information. The compositions of the electrodes were also found to remain unchanged as evidenced by PXRD patterns after chronoamperometric tests, as shown in Figure S6. These studies further confirmed that the $Ni_3Te_2$ electrodes were indeed stable for long-term glucose oxidation with no structural or morphological degradation.

**Human Blood Glucose Determination.** To verify the possibility of the $Ni_3Te_2$ sensor in practical application, $Ni_3Te_2$–NF electrode was used to test human blood glucose concentration. As provided in Table S1, $Ni_3Te_2$ sensor shows excellent performance toward glucose detection in physiological blood samples. To quantify the glucose level in blood samples, first, the human blood samples obtained from three participating volunteers were tested with the commercially



DOI: 10.1021/acsomega.9b01063
ACS Omega 2019, 4, 11152−11162

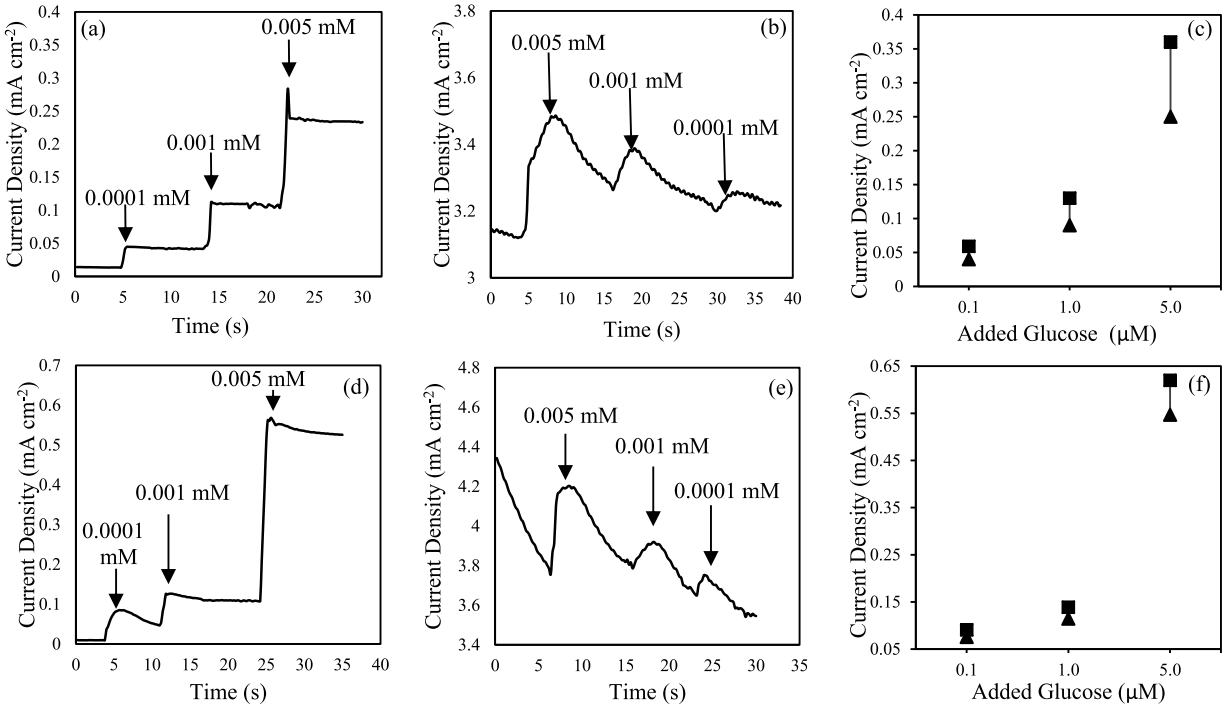


**Figure 6.** (a) Successive addition of 0.1, 1, and 5 $\mu$M of glucose to 0.1 M KOH (using electrodeposited $Ni_3Te_2$). (b) Reverse injections of 5, 1, and 0.1 $\mu$M of glucose to a 0.1 M KOH solution containing 5 mM of glucose. (c) Difference between current densities measured for electrodeposited $Ni_3Te_2$–NF electrode. (d) Stepwise addition of low concentrations of glucose to 0.1 M KOH (using hydrothermally prepared $Ni_3Te_2$–NF electrode). (e) Addition of low concentrations of glucose to a 0.1 M KOH solution containing 5 mM of glucose. (f) Difference between current densities measured for hydrothermally synthesized $Ni_3Te_2$–NF electrode.

available glucometer (ReliOn). The electrochemical test was then carried out by initially adding 100 $\mu$L of 1 mM glucose solution 2 times to the electrolyte (0.05 M KOH) to stabilize the system's current response. Then, 100 $\mu$L of the human blood sample was directly injected into the 0.05 M KOH followed by two more additions of 1 mM glucose. The current response for each of the standard glucose additions (i.e., 1 mM glucose solution) was recorded and plotted as a function of concentration producing a linear plot, as shown in Figure S7. The level of the glucose present in the blood sample was estimated from the linear fit of the plot (after subtracting the background glucose concentrations).[64] As shown in Table S1, the glucose concentration measured with $Ni_3Te_2$-based sensor, regardless of the fabrication method, was in good agreement with the results obtained from the commercial glucometer, confirming the possibility of $Ni_3Te_2$ as a promising sensor for human blood glucose testing.

Another growing emphasis for nonenzymatic glucose, especially with respect to the continuous glucose monitoring system, is to develop sensors that can detect very low amounts of glucose present in other bodily fluids such as sweat, urine, tears, tissue fluid, etc. Detecting sudden spikes in glucose levels is also important to control diabetes. Hence, to demonstrate the capability of the $Ni_3Te_2$ electrode for testing low concentrations of glucose, such as those that might be present in tissue and other biological fluids, different solutions containing low concentrations of glucose were prepared, and the level of glucose was tested with a commercially available glucose biosensor. Then, the glucose solutions were added to our three-electrode system to measure the current responses. As shown in Table S1, the results from both electrodeposited $Ni_3Te_2$ and hydrothermally synthesized $Ni_3Te_2$ were in good agreement with the results obtained from ReliOn glucometer. The relative standard deviation below 3.5% verified the superior electrochemical performance of $Ni_3Te_2$ as a promising candidate for an effective glucose sensing platform.

Moreover, the possibility of detecting small changes in glucose level in a glucose-enriched solution was tested. Figure 6a,d shows the injection of 0.1, 1, and 5 $\mu$M of glucose to 0.1 M KOH and the corresponding changes in current density for electrodeposited $Ni_3Te_2$, as well as hydrothermally synthesized $Ni_3Te_2$, respectively. Then, 5 mM of glucose was added to a 0.1 M KOH solution to resemble the normal glucose level in blood. Figure 6b,c demonstrates the effect of injection of 5, 1, and 0.1 $\mu$M of glucose to this alkaline solution containing 5 mM glucose for electrodeposited and hydrothermally prepared $Ni_3Te_2$, respectively. It should be noted here that small change in glucose level was detected reliably even in the presence of high glucose concentration. The difference between the current response measured from glucose addition to an alkaline medium with zero initial concentration of glucose and the injection of similar concentrations of glucose to an electrolyte containing 5 mM of glucose is compared in Figure 6c,e. It can be concluded from these figures that the standard deviation in detecting small glucose concentration reliably was small in the lower concentration range. In the higher-glucose-concentration range, detecting an accurate concentration of glucose was challenging due to the considerable background current generated by the presence of the excess amount of glucose, which reduced the availability of the active sites for a new analyte on the catalyst surface. However, $Ni_3Te_2$ electrode can successfully detect even minute amounts of increase in glucose concentration in a glucose-rich medium to a reliable extent. Such capabilities will be extremely useful to detect



DOI: 10.1021/acsomega.9b01063
ACS Omega 2019, 4, 11152−11162

spikes in glucose concentrations under physiological conditions.

To the best of our knowledge, the functional parameters for this nonenzymatic sensor based on $Ni_3Te_2$ including sensitivity, LOD, and working potential are considerably better than the previously reported sensors, as can be seen from the comparison, Table S2. It can be concluded from this table that the extremely low working potential along with ultrahigh sensitivity of $Ni_3Te_2$ validated our initial hypothesis that replacing oxides and selenides with tellurides can lower the band gap, enhance the redox activity of the Ni site, and consequently lower the applied potential to 0.35 V vs AglAgCl. From our previous research, it was also observed that $Ni_3Te_2$ surface exhibited favorable −OH adsorption kinetics on the Ni site, leading to catalyst activation at lower potential.[48] Since glucose oxidation follows catalyst activation and initiates at the $S$−OH site ($S$ = catalytically active transition-metal ion), improved catalyst activation at low applied potential will have a positive influence on enhancing the glucose oxidation catalytic activity. The low working potential can overcome one of the biggest challenges associated with these nonenzymatic sensors, which is the selectivity of the electrode toward glucose oxidation. This modest working potential will make $Ni_3Te_2$ an ideal candidate for smaller, economical, and energy-efficient glucometers.

## CONCLUSIONS

In this study, two convenient electrochemical synthesis processes of electrodeposition and hydrothermal synthesis were employed to prepare $Ni_3Te_2$ nanostructures on Ni foam. The morphology, composition, and electrocatalytic performance of the binder-free electrodes were carefully characterized by various techniques. Both developed nonenzymatic sensors showed a superior catalytic activity toward the electrochemical oxidation of glucose. For electrodeposited $Ni_3Te_2$, an extremely high sensitivity of 41.615 mA $mM^{-1}$ $cm^{-2}$ with a low LOD of 0.43 $\mu$M in a range between 0.01 and 0.8 mM and 9.26 mA $mM^{-1}$ $cm^{-2}$ for the range of 1.0−4.0 mM was measured along with the other advantages associated with this electrode such as fast response, excellent selectivity, and long-term stability and repeatability. The hydrothermally synthesized $Ni_3Te_2$ electrode also provides a high sensitivity of 35.213 mA $mM^{-1}$ $cm^{-2}$ from 0.01 $\mu$M to 0.8 mM with an LOD as low as 0.38 $\mu$M and 9.802 mA $mM^{-1}$ $cm^{-2}$ from 1 to 4 mM. Excellent selectivity, reproducibility of current response, and long-term functional stability of this electrode verified the intrinsic properties of $Ni_3Te_2$ toward glucose sensing through direct electrooxidation. It can be concluded that $Ni_3Te_2$ is a potential material for the development of an enzyme-free sensor for reliable glucose determination.

## EXPERIMENTAL SECTION

All chemicals used in this research were used as purchased, without further purification. Nickel sulfate ($NiSO_4·6H_2O$) was purchased from Fisher Scientific, and tellurium dioxide ($TeO_2$) and hydrazine hydrate ($N_2H_4·H_2O$) were purchased from Acros Organics. Dextrose and dopamine were purchased from Sigma-Aldrich, ascorbic acid, sodium chloride, potassium chloride, and lactose were obtained from Fisher Scientific, and fructose from Sigma-Aldrich. Ni foam was employed as a substrate in both electrodeposition and hydrothermal synthesis. Deionized water (DI water) was used to prepare all of the solutions. Ni foam was rinsed with dilute HCl and DI water prior to the preparation of $Ni_3Te_2$ electrode.

**Electrodeposition of $Ni_3Te_2$.** Direct electrodeposition was carried out in a conventional three-electrode system using an IviumStat potentiostat, with Ni foam as the working electrode, Pt as the counter electrode, and AglAgCl as the reference electrode. The electrolyte contained 15 mM of nickel sulfate and 3 mM of tellurium dioxide and was maintained at 80 °C with a pH of 2.5 by the addition of dilute HCl. $Ni_3Te_2$ was deposited on precleaned Ni foam at −1.05 V (vs AglAgCl).

**Hydrothermal Synthesis of $Ni_3Te_2$.** $NiSO_4·6H_2O$ (9.0 mM) was dissolved in 15.0 mL of deionized water under vigorous magnetic stirring. Then, $TeO_2$ (6.0 mM) was added to the reaction mixture and stirred for 20 min to form a homogeneous solution. Finally, $N_2H_4·H_2O$ (3.0 mL) was added to the mixture and stirred continuously for another 10 min. The resulting solution was transferred into a Teflon-lined stainless steel autoclave. Precleaned Ni foam was placed inside the autoclave, which was sealed and maintained at 185 °C for 20 h. Later, it was naturally cooled down to room temperature. The prepared electrode was washed several times with DI water to remove impurities. The product was dried in a vacuum oven at 60 °C for 24 h.

A detailed description of the synthesis procedure and morphological and structural studies has been reported in our previous work.[48]

## CHARACTERIZATION

**Powder X-ray Diffraction (PXRD).** The obtained electrodeposited and hydrothermally synthesized $Ni_3Te_2$ samples were characterized by powder X-ray diffraction measurements using a Philips X-Pert X-ray diffractometer (PANalytical, Almelo, The Netherlands, $\lambda$ = 1.5418 Å). The PXRD pattern was collected from 2$\theta$ values of 10−90°.

**Scanning Electron Microscopy (SEM).** SEM images of $Ni_3Te_2$ were acquired using an FEI Helios NanoLab 600 FIB/FESEM operating at an acceleration voltage of 10 kV and a working distance of 5.0 mm to study the morphology of the product.

## ASSOCIATED CONTENT

### Supporting Information

The Supporting Information is available free of charge on the ACS Publications website at DOI: 10.1021/acsomega.9b01063.

ECSA plots; cyclic voltammetry of Ni foam in the absence and presence of glucose; EIS results of electrodeposited $Ni_3Te_2$; real-life application; SEM image and PXRD pattern of $Ni_3Te_2$ after chronoamperometric tests; and comparison table (PDF)

## AUTHOR INFORMATION

### Corresponding Author

*E-mail: nathm@mat.edu.

### ORCID

Manashi Nath: 0000-0002-5058-5313

### Notes

The authors declare no competing financial interest.



DOI: 10.1021/acsomega.9b01063
ACS Omega 2019, 4, 11152−11162

## ■ ACKNOWLEDGMENTS

M.N. and J.M. would like to thank the NSF for financial support. The authors would also like to thank the Materials Research Center for equipment usage.

## ■ REFERENCES

(1) Qian, Q.; Hu, Q.; Li, L.; Shi, P.; Zhou, J.; Kong, J.; Zhang, X.; Sun, G.; Huang, W. Sensitive fiber microelectrode made of nickel hydroxide nanosheets embedded in highly-aligned carbon nanotube scaffold for nonenzymatic glucose determination. *Sens. Actuators, B* **2018**, *257*, 23−28.

(2) Kim, S.; Lee, S. H.; Cho, M.; Lee, Y. Solvent-assisted morphology confinement of a nickel sulfide nanostructure and its application for non-enzymatic glucose sensor. *Biosen. Bioelectron.* **2016**, *85*, 587−595.

(3) Nichols, S. P.; Koh, A.; Storm, W. L.; Shin, J. H.; Schoenfisch, M. H. Biocompatible materials for continuous glucose monitoring devices. *Chem. Rev.* **2013**, *113*, 2528.

(4) Turner, A. P. F. Biosensors: sense and sensibility. *Chem. Soc. Rev.* **2013**, *42*, 3184−3196.

(5) Tian, K.; Prestgard, M.; Tiwari, A. A review of recent advances in nonenzymatic glucose sensors. *Mater. Sci. Eng., C* **2014**, *41*, 100−118.

(6) Bandodkar, A. J.; Wang, J. Non-invasive wearable electrochemical sensors: a review. *Trends Biotechnol.* **2014**, *32*, 363−371.

(7) Hammock, M. L.; Chortos, A.; Tee, B. C.-K.; Tok, J. B.-H.; Bao, Z. The evolution of electronic skin (e-skin): a brief history, design considerations, and recent progress. *Adv. Mater.* **2013**, *25*, 5997−6038.

(8) Windmiller, J. R.; Wang, J. Wearable electrochemical sensors and biosensors: a review. *Electroanalysis* **2013**, *25*, 29−46.

(9) Lankelma, J.; Nie, Z.; Carrilho, E.; Whitesides, G. M. Paper-Based Analytical Device for Electrochemical Flow-Injection Analysis of Glucose in Urine. *Anal. Chem.* **2012**, *84*, 4147−4152.

(10) Ye, D.; Liang, G.; Li, H.; Luo, J.; Zhang, S.; Chen, H.; Kong, J. A novel nonenzymatic sensor based on CuO nanoneedle/graphene/carbon nanofiber modified electrode for probing glucose in saliva. *Talanta* **2013**, *116*, 223−230.

(11) Moyer, J.; Wilson, D.; Finkelshtein, I.; Wong, B.; Potts, R. Correlation between sweat glucose and blood glucose in subjects with diabetes. *Diabetes Technol. Ther.* **2012**, *14*, 398−402.

(12) Wang, J.; Xu, L.; Lu, Y.; Sheng, K.; Liu, W.; Chen, C.; Li, Y.; Dong, B.; Song, H. Engineered $IrO_2$@NiO Core−Shell Nanowires for Sensitive Nonenzymatic Detection of Trace Glucose in Saliva. *Anal. Chem.* **2016**, *88*, 12346−12353.

(13) Ramachandran, K.; Raj Kumar, T.; Babu, K. J.; Gnana Kumar, G. Ni-Co bimetal nanowires filled multiwalled carbon nanotubes for the highly sensitive and selective non-enzymatic glucose sensor applications. *Sci. Rep.* **2016**, *6*, No. 36583.

(14) Ronkainen, N. J.; Halsall, H. B.; Heineman, W. R. Electrochemical biosensors. *Chem. Soc. Rev.* **2010**, *39*, 1747−1763.

(15) Liu, S.; Ma, Y.; Cui, M.; Luo, X. Enhanced electrochemical biosensing of alpha-fetoprotein based on three-dimensional macroporous conducting polymer polyaniline. *Sens. Actuators, B* **2018**, *255*, 2568−2574.

(16) Bao, S. J.; Li, C. M.; Zang, J. F.; Cui, X. Q.; Qiao, Y.; Guo, J. New nanostructured $TiO_2$ for direct electrochemistry and glucose sensor applications. *Adv. Funct. Mater.* **2008**, *18*, 591−599.

(17) Tee, S. Y.; Teng, C. P.; Ye, E. Metal nanostructures for non-enzymatic glucose sensing. *Mater. Sci. Eng., C* **2017**, *70*, 1018−1030.

(18) Wang, G.; He, X.; Wang, L.; Gu, A.; Huang, Y.; Fang, B.; Geng, B.; Zhang, X. Non-enzymatic electrochemical sensing of glucose. *Microchim. Acta* **2013**, *180*, 161−186.

(19) Huang, W.; Cao, Y.; Chen, Y.; Peng, J.; Lai, X.; Tu, J. Fast synthesis of porous $NiCo_2O_4$ hollow nanospheres for a high-sensitivity non-enzymatic glucose sensor. *Appl. Surf. Sci.* **2017**, *396*, 804−811.

(20) Rajendran, S.; Manoj, D.; Raju, K.; Dionysiou, D. D.; Naushad, M.; Gracia, F.; Cornejo, L.; Gracia-Pinilla, M. A.; Ahamad, T. Influence of mesoporous defect induced mixed-valent NiO($Ni^{2+}$/$Ni^{3+}$)-$TiO_2$ nanocomposite for non-enzymatic glucose biosensors. *Sens. Actuators, B* **2018**, *264*, 27−37.

(21) Benjamin, M.; Manoj, D.; Thenmozhi, K.; Bhagat, P. R.; Saravanakumar, D.; Senthilkumar, S. A bioinspired ionic liquid tagged cobalt-salophen complex for nonenzymatic detection of glucose. *Biosens. Bioelectron.* **2017**, *91*, 380−387.

(22) Si, P.; Huang, Y.; Wang, T.; Ma, J. Nanomaterials for electrochemical non-enzymatic glucose biosensors. *RSC Adv.* **2013**, *3*, 3487.

(23) Tian, K.; Prestgard, M.; Tiwari, A. A review of recent advances in non-enzymatic glucose sensors. *Mater. Sci. Eng., C* **2014**, *41*, No. 100118.

(24) Toghill, K. E.; Compton, R. G. Electrochemical Non-enzymatic Glucose Sensors: A Perspective and an Evaluation. *Int. J. Electrochem. Sci.* **2010**, *5*, 1246−1301.

(25) Zhu, Z.; Gancedo, L. G.; Flewitt, A. J.; Xie, H.; Moussy, F.; Milne, W. I. A critical review of glucose biosensors based on carbon nanomaterials: carbon nanotubes and graphene. *Sensors* **2012**, *12*, 5996−6022.

(26) Han, L.; Zhang, S.; Han, L.; Yang, D.-P.; Hou, C.; Liu, A. Porous gold cluster film prepared from Au@BSA microspheres for electrochemical nonenzymatic glucose sensor. *Electrochim. Acta* **2014**, *138*, 109−114.

(27) Fu, S.; Fan, G.; Yang, L.; Li, F. Non-enzymatic glucose sensor based on Au nanoparticles decorated ternary Ni-Al layered double hydroxide/single-walled carbon nanotubes/graphene nanocomposite. *Electrochim. Acta* **2015**, *152*, 146−154.

(28) Shen, N.; Xu, H.; Zhao, W.; Zhao, Y.; Zhang, X. Highly Responsive and Ultrasensitive Non-Enzymatic Electrochemical Glucose Sensor Based on Au Foam. *Sensors* **2019**, *19*, No. 1203.

(29) Shim, K.; Lee, W.-C.; Park, M.-S.; Shahabuddin, M.; Yamauchi, Y.; Hossain, S. A.; Shim, Y.-B.; Kim, J. H. Au decorated core-shell structured Au@Pt for the glucose oxidation reaction. *Sens. Actuators, B* **2019**, *278*, 88−96.

(30) Shen, C.; Su, J.; Li, X.; Luo, J.; Yang, M. Electrochemical sensing platform based on Pd−Au bimetallic cluster for non-enzymatic detection of glucose. *Sens. Actuators, B* **2015**, *209*, 695−700.

(31) Lee, S.; Lee, J.; Park, S.; Boo, H.; Kim, H. C.; Chung, T. D. Disposable non-enzymatic blood glucose sensing strip based on nanoporous platinum particles. *Appl. Mater. Today* **2018**, *10*, 24−29.

(32) Hoa, L. T.; Sun, K. G.; Hur, S. H. Highly sensitive non-enzymatic glucose sensor based on Pt nanoparticle decorated graphene oxide hydrogel. *Sens. Actuators, B* **2015**, *210*, 618−623.

(33) Wu, Y.-S.; Wu, Z.-W.; Lee, C.-L. Concave Pd core/island Pt shell nanoparticles: Synthesis and their promising activities toward neutral glucose oxidation. *Sens. Actuators, B* **2019**, *281*, 1−7.

(34) Ye, J.-S.; Chen, C.-W.; Lee, C.-L. Pd nanocube as non-enzymatic glucose sensor. *Sens. Actuators, B* **2015**, *208*, 569−574.

(35) Wang, L.; Lu, X.; Wen, C.; Xie, Y.; Miao, L.; Chen, S.; Li, H.; Li, P.; Song, Y. One-step synthesis of Pt−NiO nanoplate array/reduced graphene oxide nanocomposites for nonenzymatic glucose sensing. *J. Mater. Chem. A* **2015**, *3*, 608−616.

(36) Madhu, R.; Veeramani, V.; Chen, S. M.; Manikandan, A.; Lo, A. Y.; Chueh, Y. L. Honeycomb-like porous carbon-cobalt oxide nanocomposite for high-performance enzyme-less glucose sensor and supercapacitor applications. *ACS Appl. Mater. Interfaces* **2015**, *7*, 15812−15820.

(37) Xie, F.; Liub, T.; Xieb, L.; Sunb, X.; Luo, Y. Metallic nickel nitride nanosheet: An efficient catalyst electrode for sensitive and selective non-enzymatic glucose sensing. *Sens. Actuators, B* **2018**, *255*, 2794−2799.

(38) Fang, Y.; Li, C.; Bo, J.; Henzie, J.; Yamauchi, Y.; Asahi, T. Chiral sensing with mesoporous Pd@Pt nanoparticles. *ChemElectroChem* **2017**, *4*, 1832−1835.

(39) Hsu, C.; Lin, J.; Hsu, D.; Wang, S.; Lin, S.; Hsueh, T. Enhanced non-enzymatic glucose biosensor of ZnO nanowires via decorated Pt



DOI: 10.1021/acsomega.9b01063
*ACS Omega* 2019, 4, 11152−11162

nanoparticles and illuminated with UV/green light emitting diodes. *Sens. Actuators, B* **2017**, *238*, 150−159.
(40) Tekbaşoğlu, T. Y.; Soganci, T.; Ak, M.; Koca, A.; Sener, M. K. Enhancing biosensor properties of conducting polymers via copolymerization: synthesis of EDOT-substituted bis(2-pyridylimino) isoindolato-palladium complex and electrochemical sensing of glucose by its copolymerized film. *Biosens. Bioelectron.* **2017**, *87*, 81−88.
(41) He, G.; Tian, L.; Cai, Y.; Wu, S.; Su, Y.; Yan, H.; Pu, W.; Zhang, J.; Li, L. Sensitive Nonenzymatic Electrochemical Glucose Detection Based on Hollow Porous NiO. *Nanoscale Res. Lett.* **2018**, *13*, No. 3.
(42) Wang, L.; Ye, Y.; Shen, Y.; Wang, F.; Lu, X.; Xie, Y.; Chen, S.; Tan, H.; Xu, F.; Song, Y. Hierarchical nanocomposites of Co3O4/polyaniline nanowire arrays/reduced graphene oxide sheets for amino acid detection. *Sens. Actuators, B* **2014**, *203*, 864−872.
(43) Liu, T.; Lib, M.; Dong, P.; Zhang, Y.; Zhou, M. Designing and synthesizing various nickel nitride ($Ni_3N$) nanosheets dispersed carbon nanomaterials with different structures and porosities as the high-efficiency non-enzymatic sensors. *Sens. Actuators, B* **2018**, *260*, 962−975.
(44) Chen, C.; Shi, M.; Xue, M.; Hu, Y. Synthesis of nickel (II) coordination polymers and conversion into porous NiO nanorods with excellent electrocatalytic performance for glucose detection. *RSC Adv.* **2017**, *7*, 22208−22214.
(45) Toghill, K. E.; Xiao, L.; Phillips, M. A.; Compton, R. G. The non-enzymatic determination of glucose using an electrolytically fabricated nickel microparticle modified boron-doped diamond electrode or nickel foil electrode. *Sens. Actuators, B* **2010**, *147*, 642.
(46) Garcia-Garcia, F. J.; Salazar, P.; Yubero, F.; González-Elipe, A. R. Non-enzymatic Glucose electrochemical sensor made of porous NiO thin films prepared by reactive magnetron sputtering at oblique angles. *Electrochim. Acta* **2016**, *201*, 38−44.
(47) Safavi, A.; Maleki, N.; Farjami, E. Fabrication of a glucose sensor based on a novel nanocomposite electrode. *Biosens. Bioelectron.* **2009**, *24*, 1655−1660.
(48) De Silva, U.; Masud, J.; Zhang, N.; Hong, Y.; Liyanage, W. P. R.; Asle Zaeem, M.; Nath, M. Nickel telluride as a bifunctional electrocatalyst for efficient water splitting in alkaline medium. *J. Mater. Chem. A* **2018**, *6*, 7608−7622.
(49) Amin, B. G.; Swesi, A. T.; Masud, J.; Nath, M. $CoNi_2Se_4$ as an efficient bifunctional electrocatalyst for overall water splitting. *Chem. Commun.* **2017**, *53*, 5412−5415.
(50) Masud, J.; Liyanage, W. P. R.; Cao, X.; Saxena, A.; Nath, M. Copper selenides as high-efficiency electrocatalysts for oxygen evolution reaction. *ACS Appl. Energy Mater.* **2018**, *1*, 4075−4083.
(51) Swesi, A. T.; Masud, J.; Liyanage, W. R. P.; Umapathi, S.; Bohannan, E.; Medvedeva, J.; Nath, M. textured $NiSe_2$ film: bifunctional electrocatalyst for full water splitting at remarkably low overpotential with high energy efficiency. *Sci. Rep.* **2017**, *7*, No. 2401.
(52) Yan, X.; Tian, L.; Atkins, S.; Liu, Y.; Murowchick, J.; Chen, X. Converting CoMoO4 into CoO/MoOx for Overall Water Splitting by Hydrogenation. *ACS Sustainable Chem. Eng.* **2016**, *4*, 3743−3749.
(53) Yan, X.; Tian, L.; Murowchick, J.; Chen, X. Partially amorphized $MnMoO_4$ for highly efficient energy storage and the hydrogen evolution reaction. *J. Mater. Chem. A* **2016**, *4*, 3683−3688.
(54) Yan, X.; Li, K.; Lyu, L.; Song, F.; He, J.; Niu, D.; Liu, L.; Hu, X.; Chen, X. From Water Oxidation to Reduction: Transformation from NixCo3−xO4Nanowires to NiCo/NiCoOx Heterostructures. *ACS Appl. Mater. Interfaces* **2016**, *8*, 3208−3214.
(55) Shen, L.; Wang, J.; Xu, G.; Li, H.; Dou, H.; Zhang, X. $NiCo_2S_4$ nanosheets grown on nitrogen-doped carbon foams as an advanced electrode for supercapacitors. *Adv. Energy Mater.* **2015**, *5*, No. 1400977.
(56) Wang, S.; Li, W.; Xin, L.; Wu, M.; Long, Y.; Huang, H.; Lou, X. Facile synthesis of truncated cube-like $NiSe_2$ single crystals for high-performance asymmetric supercapacitors. *Chem. Eng. J.* **2017**, *330*, 1334−1341.
(57) Shamsipur, M.; Najafi, M.; Hosseini, M. R. Highly improved electrooxidation of glucose at a nickel (II) oxide/multi-walled carbon nanotube modified glassy carbon electrode. *Bioelectrochemistry* **2010**, *77*, 120−124.
(58) Mani, S.; Ramaraj, S.; Chen, S.-M.; Dinesh, B.; Chen, T.-W. Two-dimensional metal chalcogenides analogous $NiSe_2$ nanosheets and its efficient electrocatalytic performance towards glucose sensing. *J. Colloid Interface Sci.* **2017**, *507*, 378−385.
(59) Li, G.; Huo, H.; Xu, C. $Ni_{0.31}Co_{0.69}S_2$ nanoparticles uniformly anchored on a porous reduced graphene oxide framework for a high-performance non-enzymatic glucose sensor. *J. Mater. Chem. A* **2015**, *3*, 4922−4930.
(60) Liu, J.; Lv, W.; Wei, W.; Zhang, C.; Li, Z.; Li, B.; Kang, F.; Yang, Q.-H. A three-dimensional graphene skeleton as a fast electron and ion transport network for electrochemical applications. *J. Mater. Chem. A* **2014**, *2*, 3031−3037.
(61) Zhan, B.; Liu, C.; Chen, H.; Shi, H.; Wang, L.; Chen, P.; Huang, W.; Dong, X. Free-standing electrochemical electrode based on Ni $(OH)_2$/3D graphene foam for nonenzymatic glucose detection. *Nanoscale* **2014**, *6*, 7424−7429.
(62) Oncescu, V.; Erikson, D. High volumetric power density, non-enzymatic, glucose fuel cells. *Sci. Rep.* **2013**, *3*, No. 1226.
(63) Kerzenmacher, S.; Ducrée, J.; Zengerlea, R.; von Stetten, F. Energy harvesting by implantable abiotically catalyzed glucose fuel cells. *J. Power Sources* **2008**, *182*, 1−17.
(64) Su, C.-H.; Sun, C.-L.; Peng, S.-Y.; Wu, J.-J.; Huang, Y.-H.; Liao, Y.-C. High performance non-enzymatic graphene-based glucose fuel cell operated under moderate temperatures and a neutral solution. *J. Taiwan Inst. Chem. Eng.* **2019**, *95*, 48−54, DOI: 10.1016/j.jtice.2018.09.034.
(65) Zhao, Y.; Fan, L.; Gao, D.; Ren, J.; Hong, B. High-power non-enzymatic glucose biofuel cells based on three-dimensional platinum nanoclusters immobilized on multiwalled carbon nanotubes. *Electrochim. Acta* **2014**, *145*, 159−169.
(66) Zhang, L.; Ding, Y.; Li, R.; Ye, C.; Zhao, G.; Wang, Y. Ni-Based metal−organic framework derived Ni@C nanosheets on a Ni foam substrate as a supersensitive non-enzymatic glucose sensor. *J. Mater. Chem. B* **2017**, *5*, 5549−5555.
(67) Amin, B. G.; Masud, J.; Nath, M. Non-enzymatic glucose sensor based on $CoNi_2Se_4$/rGO nanocomposite with Ultrahigh sensitivity at low working potential. *J. Mater. Chem. B* **2019**, *7*, 2338−2348.
(68) Tian, K.; Prestgard, M.; Tiwari, A. A review of recent advances in nonenzymatic glucose sensors. *Mater. Sci. Eng., C* **2014**, *41*, 100−118.
(69) Niu, X.; Lan, M.; Zhao, H.; Chen, C. Highly Sensitive and Selective Nonenzymatic Detection of Glucose Using Three-Dimensional Porous Nickel Nanostructures. *Anal. Chem.* **2013**, *85*, 3561−3569.


DOI: 10.1021/acsomega.9b01063
*ACS Omega* 2019, 4, 11152−11162